Archives of Mechanics • Archiwum Mechaniki Stosowanej • 28, 5–6, pp. 1025–1037, Warszawa 1976

Two-dimensional, two-phase flows in a Laval nozzle with nonequilibrium phase transition

M. BRATOS and G. E. A. MEIER (WARSZAWA, GÖTTINGEN)

IN THIS paper the two-dimensional, two-phase flows with nonequilibrium phase transition are calculated using two different models of condensation: multifractional one and „surface-averaged" droplets model of condensation. The numerical results for the flows in the different nozzles are compared with experimental ones.

W pracy wyznaczono dwuwymiarowe i dwufazowe przepływy z nierównowagową przemianą fazową, stosując dwa różne modele kondensacji: wielofrakcyjny model kondensacji oraz model Hilla „średnich" kropel. Rezultaty numeryczne uzyskane dla przepływów w różnych dyszach porównano z eksperymentem.

В работе определены двухмерные и двухфазные течения с неравновесным фазовым переходом, применяя две разные модели конденсации: многофракционную модель конденсации и модель Хилла „средних" капель. Численные результаты, полученные для течений в разных соплах, сравнены с экспериментом.

Notations

ω_c mass fraction of a new phase,
ω_0 specific initial humidity,
φ relative humidity,
σ surface tension,
ϱ_d density of water (ice),
μ molecular weight,
γ ratio of specific heats,
$\mathscr{R}$ universal gas constant,
$R = \frac{\mathscr{R}}{\mu}$ specific gas constant,
p gas pressure,
T gas temperature,
ϱ gas density,
u velocity in x-direction,
v velocity in y-direction,
$\mathbf{V}$ $[u, v]$ — velocity vector of the flow,
s coordinate along a streamline,
h specific enthalpy,
r droplet radius,
$\bar{r}$ "surface-averaged" droplet radius,
r^* critical droplet radius ($r_0 \geqslant r^*$),
$\frac{dr}{dt}$ droplet growth rate,
I nucleation rate.

Subscripts

i air,
k onset of condensation,
m gas mixture of air and water vapour with suspended droplets,
o stagnation condition,
v vapour.

1. Introduction

IN OUR previous work [1–4] the analysis of steady, two-dimensional, two-phase flow in a Laval nozzle was presented. The aim of these papers was to clarify the role of two-dimensional treatment and only a very simple model of condensation was considered. In this paper we extend our previous analysis by introducing a more refined model of condensation. The physics of the considered flow can be described in a manner as outlined below (see Fig. 1).

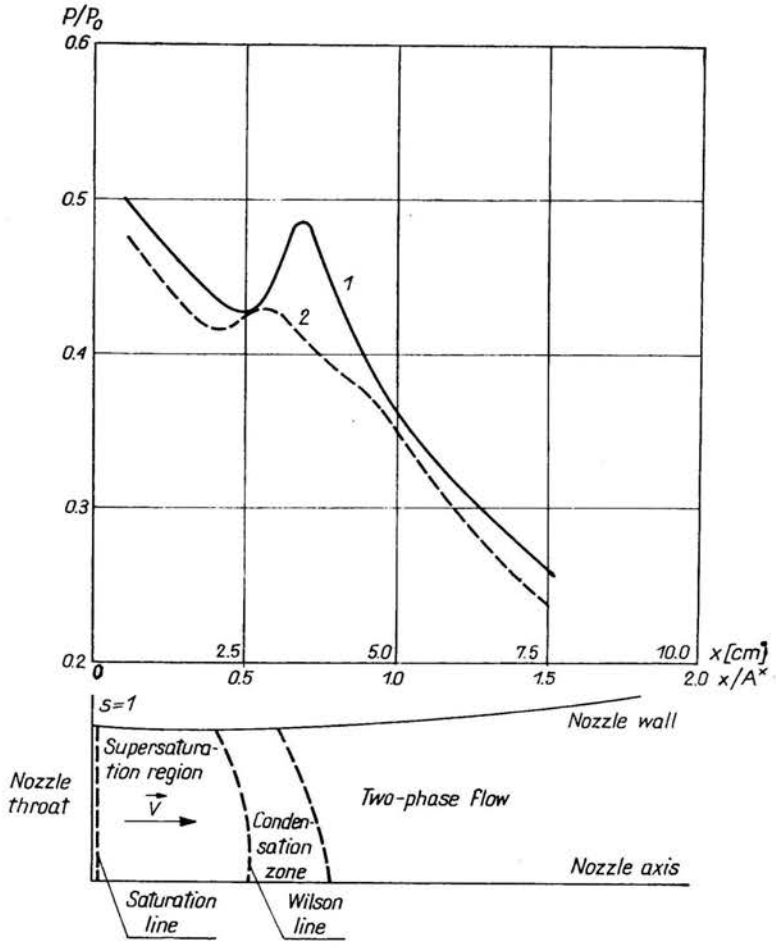

FIG. 1. The dimensionless pressure distribution along the axis (curve *1*) and along the wall of nozzle I (curve *2*); $\varphi_0 = 58\%$, $T_0 = 290.8°K$. $P_0 = 753.1$ Torr.

The moist air enters the plane nozzle from the left. Somewhere behind the throat, in the supersonic part of the nozzle flow, saturation is attained as a result of cooling the gas by its expansion. Downstream from the saturation line there is a rather extended zone in which the water vapour is supersaturated and does not condense. In this region nucleation takes place but the nucleation rate is not enough to compensate the rate of cooling due to the expansion or, to put it in other words, the relaxation time of the phase transition does not keep pace with the characteristic time of the change of the flow parameters. Hence, the flow is nearly isentropic.

With increasing supersaturation the condensation is intensified and reaches the maximal value at the so-called Wilson line, the position of which depends on the state of the entering gas and on the expansion rate.

The so-called condensation zone is defined here as a region of an intensive phase transition from the point of the maximal supersaturation to the point of thermodynamic equilibrium. The condensation zone is characterized by pressure increase in comparison with a pressure distribution for the isentropic flow.

In both the supersaturated region and in the condensation zone the thermodynamical equilibrium is lost and it is restored downstream in the region of two-phase flow.

The aim of the previous work [1–4] was to investigate the role of two-dimensional treatment. It is clear that such an approach will be in better agreement with experimental data than the one-dimensional analysis.

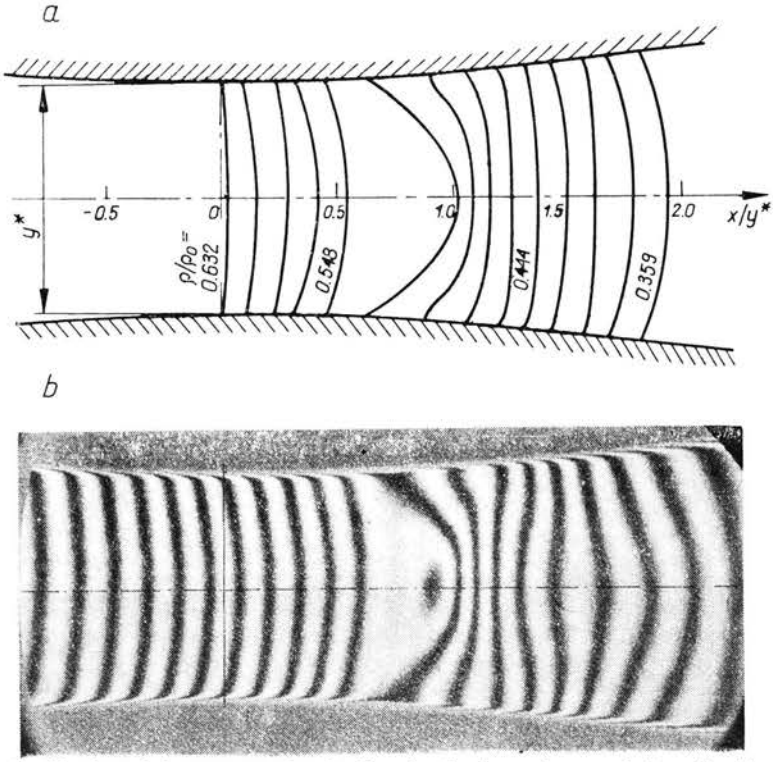

FIG. 2. The distribution of the constant density lines in the flow: a) numerical results, b) experimental ones (nozzle II); $\varphi_0 = 48.6\%$, $T_0 = 292.7°K$, $P_0 = 752$ Torr.

Figure 2 shows the theoretical distributions of the lines of constant density in the nozzle obtained by numerical computations. The calculated lines of the constant density can be compared directly with the interference fringes of Mach-Zehnder interferogram. One can see that this picture cannot be obtained in a one-dimensional treatment. In particular, the two-dimensional pattern is most pronounced in the condensation zone.

Two effects contribute to this. First, the local expansion rate at the nozzle axis is lower than that near the wall. This leads to the more marked influence of a phase transition upon the flow near the axis than near the wall. Second, the phase transition close to the wall leads to local changes of gas state and these propagate along characteristics and reach the axis in the region where condensation takes place. As was already mentioned we used a very simple model of condensation, namely the so-called "surface averaged" droplets model of condensation. Here we would like to answer the two questions. To what extent does a more realistic model of condensation influence the obtained picture of a flow? Is it possible to bypass a two-dimensional analysis with such a model of condensation? Or, in other words, is it possible to get a sufficiently precise description of a flow through a one-dimensional approach by introducing a more refined theory of condensation?

The answer to these questions can be summarized as follows — a more reliable theory of condensation does not practically influence the results obtained with the one-dimensional approach. In contrast, the results of two-dimensional computations significantly depend on the chosen model of condensation and thus, for the testing of different model of condensation, the two-dimensional approach should be used.

2. Basic model assumptions

As in the previous papers we consider a steady, two-dimensional flow of an iviscid, non-heat conducting gas (moist air) which obeys the perfect gas equation of state.

The following assumptions are used:

The mass fraction of the condensated, incompressible phase is small; the condensated phase is in the form of spherical ice clusters with uniform temperature; the ice clusters do not interact with each other and have the same speed as the bulk flow. Further, we assume that mass and energy exchange between the two phases obeys the Herz-Knudsen theory. This theory can be applied if the mean molecular free path is appreciably higher than the size of the ice clusters or water droplets.

Finally, it is assumed that full accommodation takes place. This means that the value of the thermal accommodation coefficients for the carrier gas (air) and for the water vapour are equal to 1.

In the paper mentioned earlier the Hill theory of the droplets growth was adopted. In this theory the "surface-averaged" sizes of droplets are introduced and thus the rate of growth for all droplets in a given point of the flow is the same [5–7].

In the present paper a so-called multifractional model of condensation is used and instead of averaging the size of the droplets it is assumed that their rate of growth is the function of the radius of the droplet. As nucleation takes place along the whole stream,

then, at each point of the stream droplets of different sizes can be found. Thus, for a proper description of the phenomenon the distribution function of droplet radii must be employed.

It should be mentioned that in both models, Hill's and multi-fractional ones, the Frenkel-Zeldovitch theory of nucleation is used [8–10].

3. Governing equations

Two-dimensional, steady, two-phase flow is described by the mass, momentum and energy conservation equations for a gas-solid mixture [1–3]:

$$\operatorname{div}(\varrho_m \mathbf{V}) = 0, \tag{3.1}$$

$$\varrho_m(\mathbf{V}\nabla)\mathbf{V} = -\nabla p, \tag{3.2}$$

$$\left(h_m + \frac{u^2+v^2}{2}\right)_{,s} = 0, \tag{3.3}$$

where

$$\varrho_m = \frac{\varrho}{1-\omega_c}. \tag{3.4}$$

To complete the system of equations an equation of state is required

$$p = \varrho RT, \tag{3.5}$$

where

$$R = \mathscr{R}/\mu. \tag{3.6}$$

and

$$\frac{1-\omega_0}{\mu} = \frac{1-\omega_0}{\mu_i} + \frac{(\omega_0-\omega_c)}{\mu_v}. \tag{3.7}$$

Moreover, we need an expression for the rate of formation of a new phase, i.e., equations describing nucleation and the rate of droplet growth. Droplet (cluster) growth is described by the mass and energy conservation equations for the growing droplet in the Herz-Knudsen model [3, 5, 7].

In the Hill condensation model the relative rate of formation of a new phase is given [1–5] by one integrodifferential equation:

$$\sqrt{u^2+v^2}\,\omega_{c,s} = \frac{\varrho_c}{\varrho_m}\left\{\frac{4}{3}\pi r_0^3 I(s,y) + \varrho_m\left(\frac{dr}{dt}\right)\int_0^s 4\pi\left(r_0 + \int_{s_1}^{s}\frac{dr}{dt}\frac{ds_2}{\sqrt{u^2+v^2}}\right)^2 \frac{I(s_1,y)}{\varrho_m(s_1,y)}\frac{ds_1}{\sqrt{u^2+v^2}}\right\}.$$

The first term on the right-hand side is the condensation rate due to the formation of new droplets in a fluid element at (s, y). The second term describes the condensation rate due to the growth of all droplets which have been created somewhere before a fluid element at (s, y) along the same streamline.

It should also be mentioned that, according to this expression, the droplet growth rate does not depend upon droplet size.

For the numerical integration of this equation, it is transformed into four simultaneous first-order differential equations [5–7].

In the multifractional model of condensation the relative rate of formation of a new phase is described by a more general formula

$$\sqrt{u^2+v^2}\,\omega_{c,s} = \frac{\varrho_c}{\varrho_m}\left\{\frac{4}{3}\pi r_0^3 I(s,y) + \varrho_m \int_0^s 4\pi r^2 \frac{dr}{dt}(s_1,s)\frac{I(s_1,y)}{\varrho_m(s_1,s)}\frac{ds_1}{\sqrt{u^2+v^2}}\right\}.$$

From the mathematical point of view the determination of the two-dimensional, two-phase flow in a Laval nozzle is reduced to finding the solution of the mixed problem for the set of partial differential equations of hyperbolic type.

The initial and boundary conditions for a mixed problem are formulated in the same manner as it was shown in previous papers [1–3]. Also the modified Lax scheme is used for finding the numerical solutions [1–3].

4. Results and conclusions

The numerical calculations were performed for three nozzles. The contours of nozzles I and II are given by the following expressions:

$$y = \frac{a}{b}\sqrt{x^2+b^2} \quad \text{for} \quad x \geqslant -2a, \tag{4.1}$$

$$y = \frac{a}{b}\left\{1 - \frac{2a}{4a^2+b^2}(x+2a)\right\}\sqrt{4a^2+b^2} \quad \text{for} \quad x < -2a. \tag{4.2}$$

The third nozzle has for $x < 0$ the form (4.1), (4.2); for $x > 0$ the contour is described by $y = 0.408x + 24.5$.

The values of the parameters a and b for these nozzles are listed in Table 1.

Table 1

	a[mm]	b[mm]	y^*[mm]	z[mm]
nozzle I	25	93	50	100
nozzle II	25	125	50	100
nozzle III	24.5	90	49	100

y^* is a vertex distance and z is a channel depth.

The third nozzle has the most divergent wall contour.

Figure 3 shows the results of experiments performed by M. JAESCHKE [13] and the results of numerical computations obtained using a model of condensation for the "surface-averaged" droplets. The curve of dimensionless density distribution along the nozzle axis, obtained by numerical computation for two-dimensional flow, is situated between two

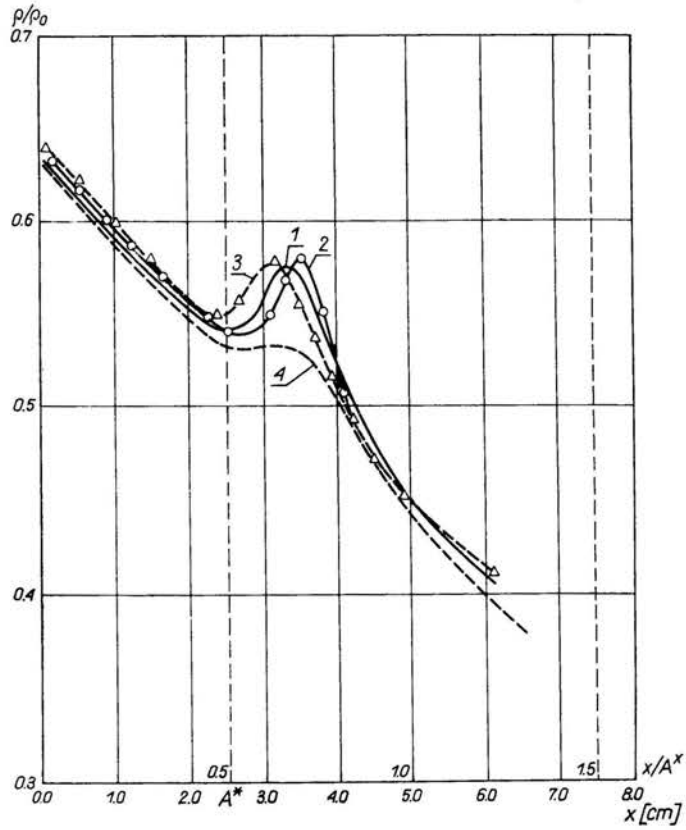

FIG. 3. The comparison of a gas density distribution for two-dimensional flow (curve *1*) with experiment (curves *2*, *3*) (axis of the nozzle I) and with the numerical results for one-dimensional flow (curve *4*); curve *1* — numerical results (two-dimensional ffow,) curve *2* — experimental results obtained from the Mach-Zehnder interferogram, curve *3* — semi-experimental results for a density calculated from pressure measurement, curve *4* — numerical results (one-dimensional flow).

density distribution curves obtained experimentally by means of different methods [3]. The distribution of the constant density lines is in good consistency with the distribution of the interference fringes (Fig. 2).

Figure 4 shows a comparison between the numerical results obtained by a "surface-averaged "droplets model (curve *1*) and the new set of values obtained using a multifractional model of condensation (curve *2*) for nozzle I.

The changes are of importance only in the condensation zone, especially along the nozzle axis. For both models the beginning of the intensive phase transition appears at the same point. The multifractional model of condensation gives, however, slower rise of the density in the condensation zone.

Also, the thermodynamical equilibrium is reached more downstream than in the case of a "surface-averaged" droplet model. This is due to the fact that for a "surface-averaged" droplet condensation model a higher percentage of larger clusters or droplets is taken into account than in a multifractional model. In a one-dimensional approach both models

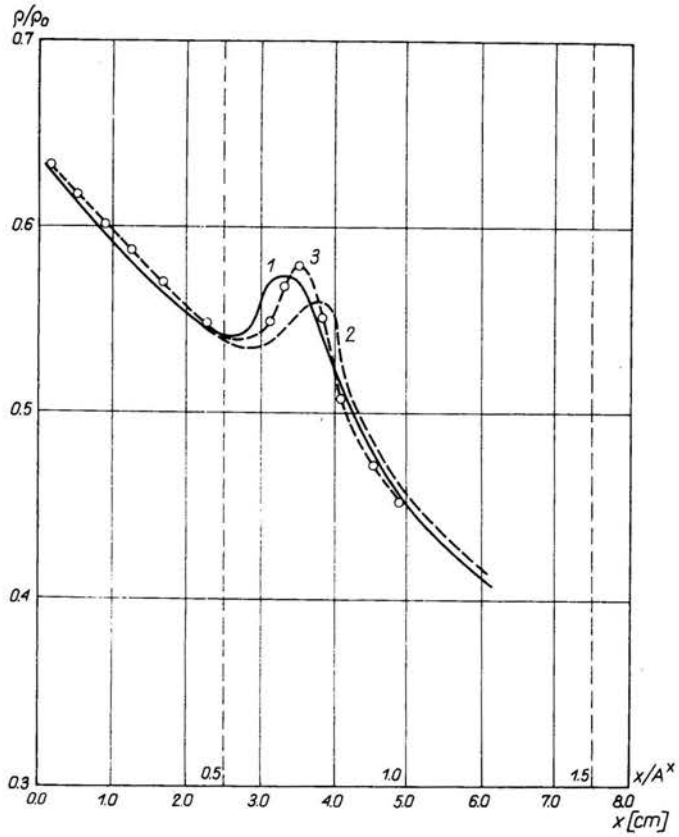

FIG. 4. The comparison of the experimental results with numerical ones obtained for two different model of condensation;
curve *1* — the dimensionless gas density distribution along the axis of nozzle I („surface-averaged" droplets model), curve *2* — the dimensionless gas density distribution along the axis of nozzle I (multifractional model of condensation), curve *3* — experimental results for the axis of nozzle I.

give almost the same results. Therefore, the use of the more reliable condensation model can give additional information about droplets growth only if one uses two-dimensional analysis.

The multifractional model of condensation gives also additional information about the distribution of droplets radii. These distributions for three points at the wall of nozzle I are shown in Fig. 5. The nonsymmetric character of the distribution is evident.

Figure 6 shows the distributions of droplets radii at the axis and at the wall of the nozzle for the same cross section ($x = 3.05$ cm) of the nozzle I.

They have the same character — nonsymmetric, but at the wall the number of smaller droplets is relatively greater than at the axis of the nozzle. The curve of the distribution of droplets sizes at the axis of the nozzle is characterized by a longer "tail" in the range of large droplets radii. This is due to the fact that along the nozzle wall the higher values of supersaturation are reached and that the condensation (nucleation) zone is wider along the axis of a nozzle than along the nozzle wall.

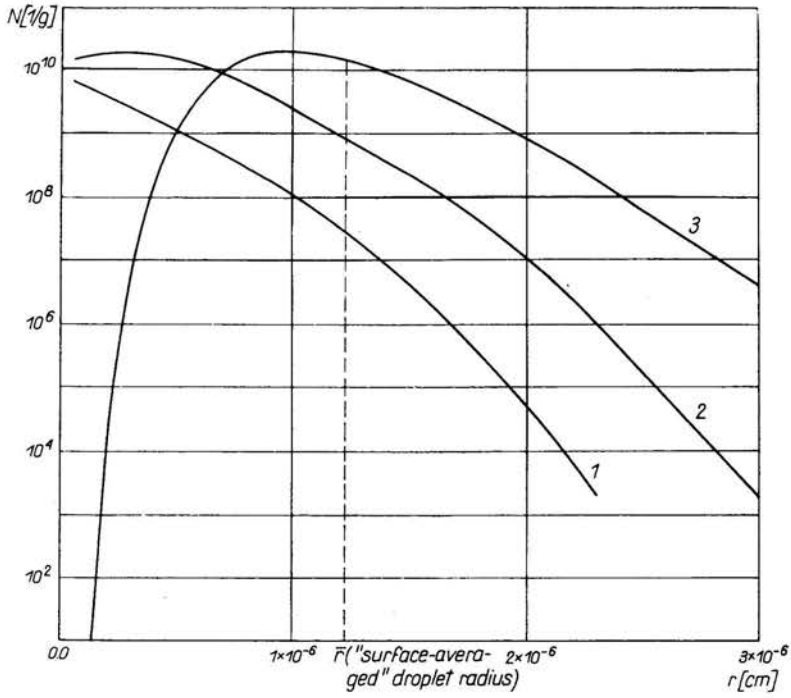

FIG. 5. The droplet sizes' distribution functions at the wall of nozzle I for: curve *1*: $x = 1.53$ cm, curve *2*: $x = 2.05$ cm, curve *3*: $x = 3{,}05$ cm.

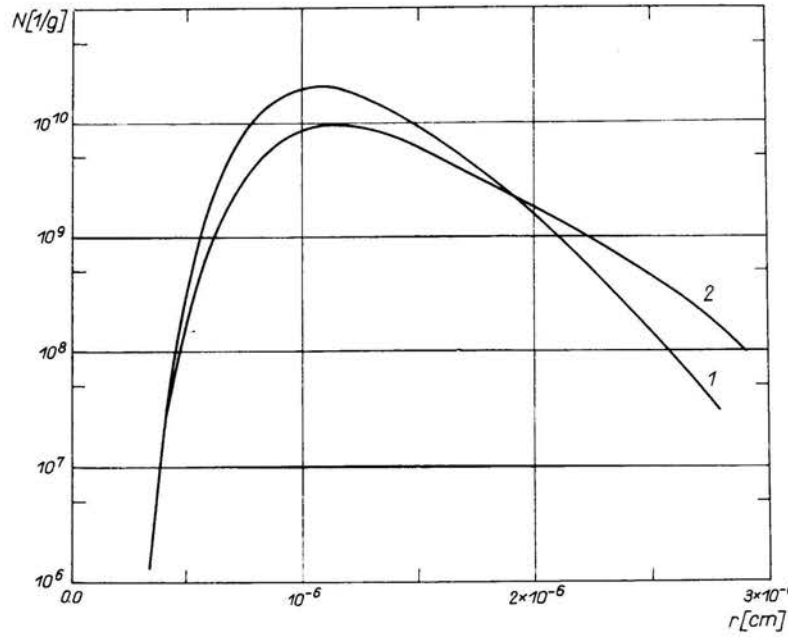

FIG. 6. The comparison between droplet sizes' distribution functions at the wall of nozzle I (curve *1*) and at the axis of nozzle I (curve *2*).

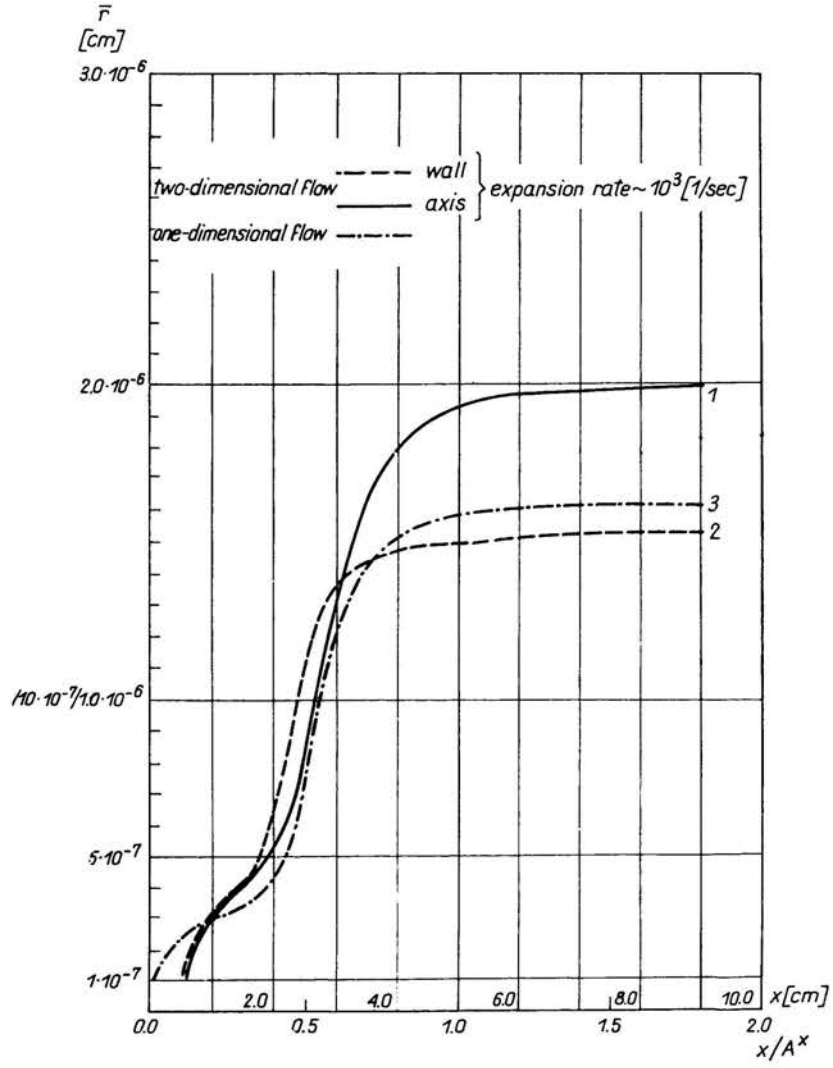

FIG. 7. The "surface-averaged" radius r distributions at the nozzle axis (curve *1*) and at the nozzle wall (curve *2*) for two-dimensional, diabatic flow and the "surface-averaged" radius r distribution for one-dimensional flow (curve *3*).

The growth of the averaged values of droplets sizes in the flow is shown in Fig. 7 (nozzle I). The difference between the averaged sizes of the droplets at the wall and at the axis is clearly marked behind the condensation zone. This difference is more pronounced for the flows with higher relative difference between the expansion rates at the nozzle wall and at the symmetry axis, at the points of maximal supersaturation.

Figures 8 and 9 illustrate the results obtained using a "surface-averaged" droplet model for the flow with condensation in nozzle III.

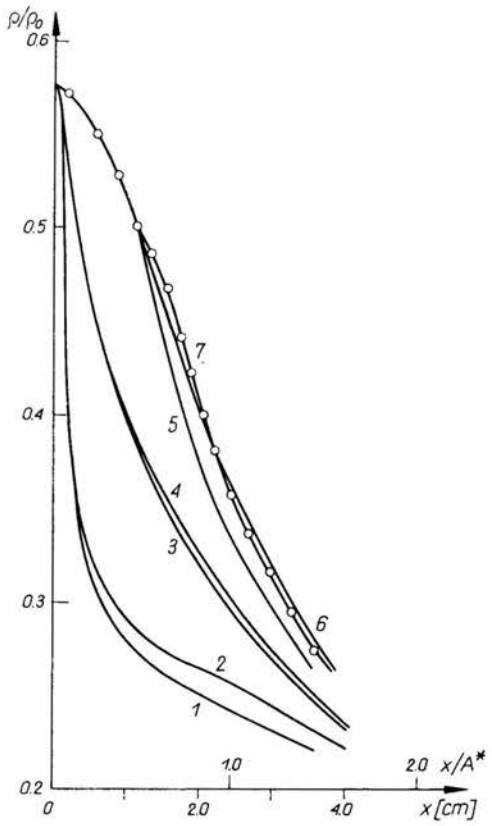

FIG. 8. The dimensionless gas density distributions along the nozzle wall (curves *1*, *2*) and along the nozzle axis (curves *5*, *6*) for two-dimensional flows in nozzle III. The dimensionless gas density distributions in one-dimensional flows for the same nozzle (curves *3*, *4*);

curves *2*, *4*, *6*, *7* — diabatic flows, curves *1*, *3*, *5* — isentropic flows, curve 7 — the experimental results for the axis of the nozzle;

$\varphi_0 = 28.3\%$, $\tau_0 = 297.6°K$, $p_0 = 751.95$ Torr.

Figure 8 shows the curves of dimensionless density distributions along the wall (curves *1* and *2*) and along the axis of the nozzle (curves *5* and *6*).

Curves *1* and *5* were obtained for an isentropic flow and curves *2*, *6* for a diabatic flow.

It is interesting to note that condensation begins at a smaller distance from the nozzle throat at the nozzle wall than at the nozzle axis (Fig. 8).

For comparison purposes the dimensionless density distributions for isentropic and diabatic flows in a one-dimensional approach are also shown by curves *3*, *4*.

The effect of the rise of a density due to the condensation is much more marked in two-dimensional flow than in the one-dimensional case.

The comparison of the results of two-dimensional treatment and the experiment shows that this is even greater that this obtained numerically in the two-dimensional approach.

This can be perhaps an indication that the condensation model should be improved.

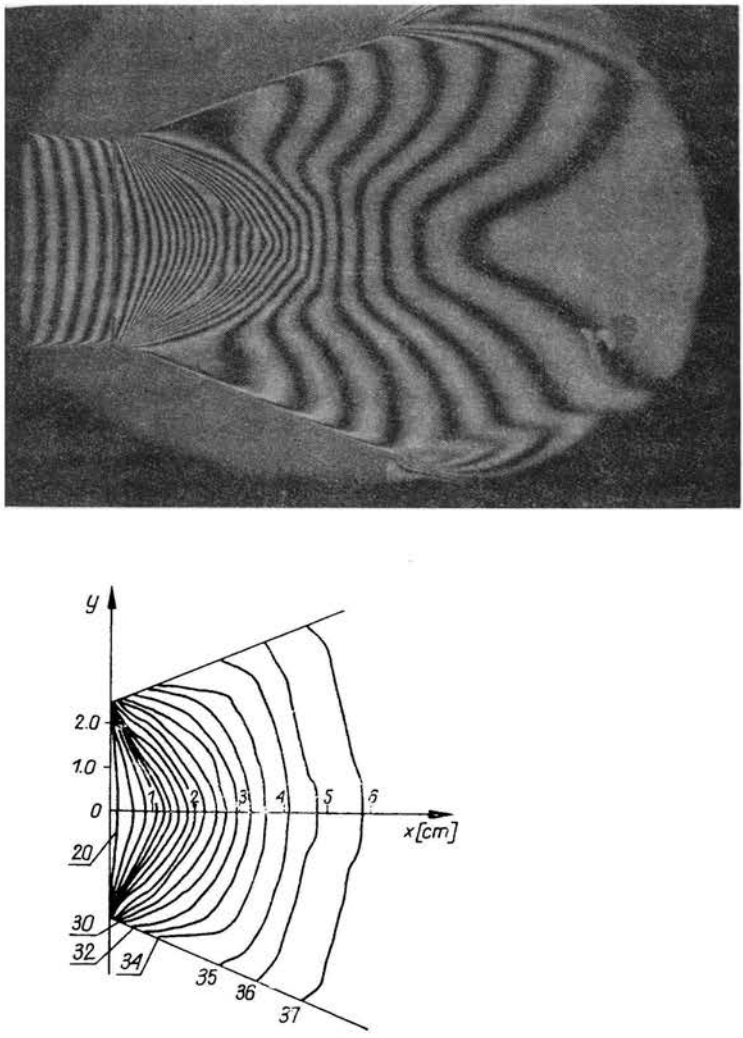

FIG. 9. The comparison between the constant density lines obtained numerically and the interference fringes obtained from the experiment (nozzle III).

The comparison between the theoretical distribution of the lines of constant density obtained numerically for nozzle III and the distribution of the interference fringes is shown in Fig. 9.

It is shown that we have a good qualitative agreement even in the case of such a highly divergent nozzle. Also, the quantitative agreement between the theory and experiment is good close to the throat of a nozzle (to about interference fringe number 35). This agreement is worse more downstream (from the interference fringe number 35). It can be attributed to several causes: first, that as it was mentioned earlier (Fig. 8) the condensation rate is greater in experiment; second, that in our calculations a uniform flow at the

throat of a nozzle is assumed, because of the presence of an angle of nozzle contour at $x = 0$; finally, the gas is treated as a perfect one.

The method of solving two-dimensional flows with condensation using the multifractional model of condensation gives satisfactory agreement with experiment. In this model a function of droplet radii distribution can be obtained. This type of analysis can be applied for testing different models of condensation.

References

1. M. BRATOS, M. BURNAT, *Two-dimensional, two-phase flow with phase transition in a de Laval nozzle*, AMS, **26**, 6, 965-979, 1974.
2. M. BRATOS, M. BURNAT, *Wpływ dwuwymiarowości na przepływ pary wodnej z kondensacją w dyszy de Lavala*, IPPT report, Warszawa 1974.
3. M. BRATOS, M. JAESCHKE, *Two-dimensional flows with non-equilibrium phase transitions*, IPPT report, Warszawa 1974.
4. M. BRATOS, B. DRZAZGOWSKA, *Zastosowanie schematu Broadbenta do dwuwymiarowego przepływu z kondensacją pary wodnej w dyszy de Lavala*, Rozpr. inżyn., **22**, 4, 645–653, 1974.
5. P. G. HILL, *Condensation of water vapour during supersonic expansion in nozzles*, J. Fluid Mech., **25**, 593, 1966.
6. D. BARSCHDORFF, *Verlauf der Zustandsgrössen und gasdynamische Zusammenhänge bei der spontanen Kondensation reinen Wasserdampfe in Lavaldüsen*, Forsch. Ing. Wes., **37**, 5, 1971.
7. P. P. WEGENER, J. A. CLUMPNER, B. J. C. WU, *Homogeneous nucleation and growth of ethanol drops in supersonic flow*, Phys. Fluid, **15**, 1869, 1972.
8. V. B. ZELDOVICH, Zh. Eksp. i Teor. Fiz., **12**, 525, 1942.
9. P. P. WEGENER (editor), *Nonequilibrium flows*, P.I. Marcel Dekker, New York and London 1969.
10. J. FRENKEL, *Kinetic theory of liquids*, Oxford Univ. Press, New York 1946.
11. G. GYARMATHY, *Spontaneous condesation phenomena. P. I. An analytical method to calculate spontaneous condensation processes*, VDI-Forsch., Heft 508, 5–30, 1965.
12. G. GYARMATHY, H. MEYER, *Spontaneous condensation phenomena, P. II. Experimental investigations on the influence of the expansion rate on the fog formation in supersaturated steam*, VDI-Forsch., Heft 508, 31–48, 1965.
13. M. JAESCHKE, *Attenuation of pressure and density fluctuations in transonic jets by condensated vapour*, Dissertation, Göttingen (1973) revised and translated version , Max-Planck-Institut für Strömungsforschung, Bericht 3, 1974.

INSTITUTE OF FUNDAMENTAL TECHNOLOGICAL RESEARCH, WARSZAWA
and
MAX-PLANCK INSTITUTE OF FLOWS RESEARCH, GÖTTINGEN.

Received February 5, 1976.